

Pleistocene iceberg production from East Greenland: Synchronous between source areas, but distinct from global ice volume

L.A. KRISSEK & K.E.K. ST. JOHN



Krissek, L.A. & St. John, K.E.K. 2002–06–26: Pleistocene iceberg production from East Greenland: Synchronous between source areas, but distinct from global ice volume. *Bulletin of the Geological Society of Denmark*, Vol. 49, pp. 79–89. Copenhagen.

A 1 m.y. ice-rafted debris record (IRD) was developed for Ocean Drilling Program site 919, located in the western Irminger Basin. Compositional analyses of the IRD indicate that the major source regions for IRD found off SE Greenland were the Precambrian igneous and meta-igneous crystalline basement (predominantly gneiss and granite) of southeast Greenland and the Tertiary flood basalts located further north along the East Greenland coast. Temporal covariations in the IRD mass accumulation rates (MARs) of provenance-distinctive grain types suggest that these source areas experienced similar iceberg release histories during the Pleistocene. In contrast, no distinct relationship can be drawn between peaks in the IRD MAR record and oxygen-isotope defined glacial-interglacial cycles, suggesting that the history of IRD input off SE Greenland since 1 Ma was dominated by local, rather than global, climatic and distributional controls.

Key words: Ice-rafted debris, Greenland, Pleistocene, Irminger Basin.

L.A. Krissek [krissek@mps.ohio-state.edu], Department of Geological Sciences, Ohio State University, Columbus, Ohio 43210, USA. K.E.K. St. John [stjohnke@appstate.edu], Department of Geology, Appalachian State University, Boone, NC 28608, USA. 13 June 2001.

The transport of land-derived sediment by icebergs, and the release of that material during iceberg melting, is widely accepted as the primary mechanism for supplying anomalously large (sand-sized and larger) land-derived grains to marine settings away from continental margins in the mid to high latitudes (e.g. Conolly & Ewing 1970; Ruddiman 1977; Krissek 1989; Jansen et al. 1990; Bond et al. 1992; Krissek 1995; Jansen et al. 2000). The temporal distribution of this material (termed “ice-rafted debris”, or IRD) at a site can be interpreted as a history of glacial extension to sea level, whereas the geographic distribution and the composition of the IRD can be used to identify the glaciated areas (e.g., Goldschmidt 1995; Linthout et al. 2000). As a result, the study of IRD in stratigraphically intact deep marine sedimentary sequences often provides a more complete record of continental glaciation than the study of thin, discontinuous stratigraphic records on the glaciated continent.

The record of IRD supply to a marine site is not without its own complications, however, because other environmental and glaciological variables can influence the rate of iceberg and IRD production and dispersal from a glacier that extends to sea level (Andrews

2000). Examples of these variables include: 1) the distribution and amount of sediment in the glacier ice, which is dependent on the basal thermal regime of the ice and the amount of bedrock exposed above the glacier surface; 2) the nature of the ice terminus (fast-calving vertical ice cliffs vs. an ice shelf or ice ramp dominated by basal melting); 3) the extent of near-shore sea ice, which restricts iceberg movement to the open ocean and enhances melting and IRD release near the iceberg source; 4) the surface current pattern in the adjacent open ocean, which acts to disperse icebergs; 5) the presence or absence of sea ice over the open ocean, which can limit iceberg movement over the site of interest; and 6) the accompanying pattern of sea surface temperatures, which determine the location and rate of enhanced iceberg melting. Changes in each of these controls through time may be difficult to distinguish, but each can affect the IRD record at an offshore marine site. Despite these complications, offshore IRD records have the potential to contribute valuable information about Pleistocene paleoenvironments of SE Greenland. Terrestrial paleoclimate records in this region are sparse and are predominantly restricted to the latest Pleistocene and Holocene (e.g., Lysa &

Landvik 1994); only two locations of early(?) Pleistocene age sediments are known to exist in East Greenland (Feyling-Hanssen et al. 1982; Funder et al 1985; and Bennike & Bøcher 1990). Fjord records provide detailed proxies (including IRD) of glacial activity in SE Greenland but are most appropriate for studying the paleoclimates of the latest Pleistocene and the Holocene (e.g. Stein et al. 1996; Andrews et al. 1997, 1998). Basal tills and depositional hiatuses in cores from the SE Greenland continental shelf (Shipboard Scientific Party 1994a) indicate that shallow water records in this region are hampered by one of the same problems found in terrestrial records – erosion by the Greenland Ice Sheet during times of maximum ice sheet extent. Hence, it is necessary to move offshore, to deeper water marine sites, to obtain a more continuous record of SE Greenland’s glacial history. Ocean Drilling Program site 919, located in the western Irminger Basin, meets this criterion. In addition, 100% core recovery (Shipboard Scientific Party 1994b), high sedimentation rates (averaging ~15 cm/ky), and age control based on oxygen-isotope stratigraphy (calibrated with calcareous nannofossil and diatom biozones; see Flower 1998) make this site attractive for high resolution paleoclimatic study of the local IRD signal from SE Greenland. In this paper, the IRD record from site 919 is used to examine: 1) the sources of IRD supplied to site 919 and the glacial histories of those source areas, and 2) the timing of local ice-rafting within Pleistocene global glacial-interglacial cycles.

Study Region and Site Description

ODP site 919 is located 185 km from the SE Greenland margin in 2088 m of water (Fig. 1). It is positioned on the lower continental rise of the western Irminger Basin. The Irminger Basin lies south of the Denmark Strait and is under the influence of the southward-flowing East Greenland Current. This cold, ice-laden current is responsible today for transporting many of the icebergs calved along East Greenland southward towards the North Atlantic. Site 919 is presently within the limit of iceberg discharge from East Greenland (Reeh 1989). Onshore, SE Greenland is characterized by numerous glacier-headed fjords that cut into the rugged alpine topography, which was uplifted during the late Oligocene and early Miocene (Larsen 1990; Christiansen et al. 1992; Shipboard Scientific Party 1994c). The highest mountains in Greenland (Gunnbjorn Fjeid, 3700 m) are located in this region, near the head of Angmagssalik Fjord ~560 km northwest of Site 919 (Funder 1989). At present the largest single outlet along the eastern margin of the Greenland Ice Sheet is

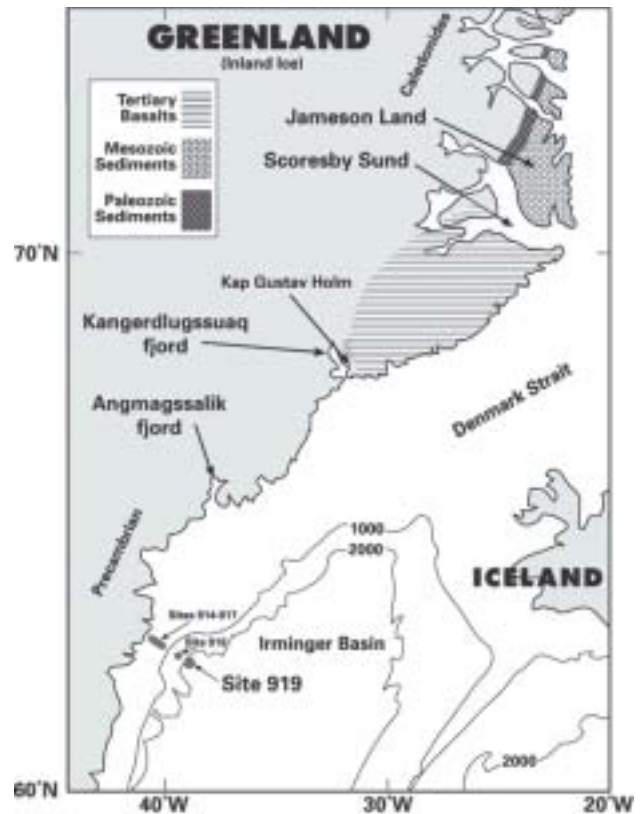


Fig. 1. Map showing the location of ODP Sites 914–919 and the general location of potential IRD source areas in SE Greenland. Bathymetric contours are in meters below sea level. Map modified from Clift et al., (1996) and Larsen (1980, 1984).

the Scoresby Sund fjord system, approximately 1000 km northeast of site 919. Funder et al. (1998) summarized modern meteorological and glaciological data for Greenland, and used data from Reeh (1991) to examine latitudinal changes in the mass balance distribution of the Greenland Ice Sheet’s eastern margin. Total ice ablation decreases significantly from south (~ 6 m/yr at sealevel at ~ 60–68°N) to north (~ 2 m/yr at sealevel at 80°N), a change reflected by modern differences in ice-terminus regimes (Reeh et al. 1999). Glaciers to the south have active ice margins that often terminate in the open sea, and ablation is dominated by the production of small irregular icebergs that carry IRD toward the open ocean. Glaciers to the north, especially those presently north of ~ 78°N, have less active margins, often ending with extended floating tongues that ablate predominantly by basal melting. These ice tongues can produce large “ice islands”, whose seaward movement is obstructed by semi-permanent fast ice. As a result, sediment load carried by the northern glaciers presently is released close to shore, rather than reaching the open ocean.

The bedrock of SE Greenland is dominated by

Precambrian gneisses and Tertiary volcanics. To a much lesser degree, Permian and Mesozoic sedimentary deposits are found in on-shore rift grabens and half-grabens, and include conglomerates, arkoses and some evaporite deposits (Larsen 1980). Pre-volcanic Tertiary sedimentary deposits are restricted to scattered localities protected against erosion by basalts (Larsen 1980). The Lodin Elv Formation, a pro-deltaic sequence on Jameson Land, north of Scoresby Sund, is the only upper Pliocene/lower Quaternary sedimentary deposit described from southeast-central East Greenland (Feyling-Hanssen et al. 1982; Funder 1989). Late Pleistocene glacial deposits blanket the landscape, and have been used by Funder et al. (1998) to investigate the history, extent, and styles of glaciation since ~ 240 ka along the relatively stable ice margin of East Greenland. Within this interval, Funder et al. (1998) have identified glacial episodes when conditions in the Scoresby Sund region were much like those presently seen north of ~ 78°N. As a result, they conclude that sustained IRD production from the Scoresby Sund region was most likely during climatic transitions, with both seasonally open water and advanced ice front positions. IRD production was reduced, however, either when ice fronts were located within the inner fjords (during warm conditions) or when permanent near-shore sea ice was present (during cold conditions). They also suggest that IRD production may have varied considerably *within* an episode of relatively stable advanced ice position if the glacier front repeatedly

oscillated across the fjord mouth, which served as a threshold for iceberg release to the open ocean.

One hundred forty-seven meters of Holocene-Pleistocene marine clays and silts with dropstones were recovered from site 919. This general lithology includes a mix of terrigenous, volcanic, and biogenic components which accumulated at site 919 from different sources and by different mechanisms. Fining upward sequences and sharp basal contacts of some silt and clay beds indicate deposition by distal turbidity flows coming off the SE Greenland shelf (Shipboard Scientific Party 1994b). Discrete ash layers were derived from fallout of explosive Icelandic volcanism (Clift & Fitton 1998; Lacasse et al. 1998). The biogenic components represent the accumulation of microfauna and flora from the overlying water column (Shipboard Scientific Party 1994b; Koç & Flower 1998; Spezzaferri 1998; Wei 1998). Most relevant to this study are the dropstones and coarse sand-sized terrigenous grains, which indicate meltout of continental material from floating ice (Shipboard Scientific Party 1994b).

Methods

The objective of this study was to generate records of the mass accumulation rate (MAR) and lithologic composition of coarse sand-sized IRD deposited at site 919 during the past 960 kyr. Samples 10 to 20 cc in volume

Table 1. Age Model for Site 919

Reference	Type	Event	Depth (mbsf)	Age (ka)	Calculated LSR (cm/kyr)
		Top of Core	0.00	10	
Flower	O-isotope stage boundary	1/2	1.50	12	75.0
	O-isotope stage boundary	2/3	2.38	24	7.3
	O-isotope stage boundary	3/4	8.00	59	16.1
	O-isotope stage boundary	4/5	10.05	71	17.1
	O-isotope stage boundary	5/6	18.90	128	15.5
	O-isotope stage boundary	6/7	27.50	186	14.8
	O-isotope stage boundary	7/8	34.76	245	12.3
	O-isotope stage boundary	8/9	41.00	303	10.8
	O-isotope stage boundary	9/10	46.00	339	13.9
	O-isotope stage boundary	10/11	48.00	362	8.7
	O-isotope stage boundary	11/12	55.50	423	12.3
	O-isotope stage boundary	12/13	64.50	478	16.4
	O-isotope stage boundary	13/14	77.90	524	29.1
	O-isotope stage boundary	14/15	85.50	565	18.5
	O-isotope stage boundary	15/16	95.60	620	18.4
	O-isotope stage boundary	16/17	103.65	670	16.1
	O-isotope stage boundary	17/18	109.00	713	12.4
	magnetostratigraphy ¹	Brunhes/Matuyama	120.50	780	17.2
	O-isotope stage boundary	24/25	146.00	953	14.7

¹Flower (personal communication) magnetostratigraphic reference: Wei (1998)

were taken approximately every 50 to 75 cm from the Pleistocene composite sequences of ODP Holes 919A and 919B. Variations in sample spacing reflect changes in core recovery and the effort to avoid basal turbidites and discrete ash layers during sampling. A total of 285 samples were processed from site 919 cores. Sample ages were determined by linear interpolation between oxygen-isotope stage boundaries (Flower 1998), assuming a constant sedimentation rate between each pair of these dated levels (Table 1). Sedimentation rates for the last 960 kyr vary, but average ~15 cm/kyr. Sedimentation rates were very high (75 cm/kyr) during the last deglaciation, between 12 and 10 ka. Given the sample spacing and the linear sedimentation rates, the average temporal resolution for this study is approximately 3 kyr.

Samples were processed with laboratory methods similar to those used previously in other IRD studies (Krissek 1989, 1995; St. John & Krissek 1999). This procedure involved isolating the coarse sand fraction (250 μm to 2 mm), weighing it, and visually estimating the relative abundance of the terrigenous (non-volcanic) material in that coarse-sand fraction. In this study, the terrigenous coarse sand fraction is used as an indicator of IRD abundance. A detailed description of the laboratory methods used can be found in Krissek (1999).

IRD compositions were determined by point counting 100 terrigenous grains per sample. However, if a sample contained <100 IRD grains then all IRD grains were counted. Grains were classified as quartz (monocrystalline and polycrystalline), basalt (black to dark green, fine-grained igneous grains), granite/coarse-grained felsic (coarse-grained, quartz-bearing, polycrystalline igneous and metamorphic grains), coarse-grained mafic (black to dark green, coarse-grained igneous and metamorphic grains), sedimentary non-carbonate and sedimentary carbonate.

We used mass accumulation rates (MARs) to quantify the total IRD flux and the fluxes of different IRD grain types (e.g., basalt grains) to the western Irminger Basin. The terrigenous coarse-sand (i.e., IRD) MAR is preferred as a glacial proxy over simple abundances of coarse sand because the IRD MAR is independent of the supply rates of other coarse-sand size components, such as volcanic ash and biogenic material. For this reason, it yields a more unequivocal record of IRD supply than is provided by the abundance of coarse sand. In addition, since LSR values vary at site 919, MARs give a clearer indication of IRD variations; for example, IRD peaks deposited during times of highest LSR generally indicate much larger debris inputs than peaks with similar weight percent values deposited during times of lower LSRs.

The total IRD MAR is calculated by multiplying the

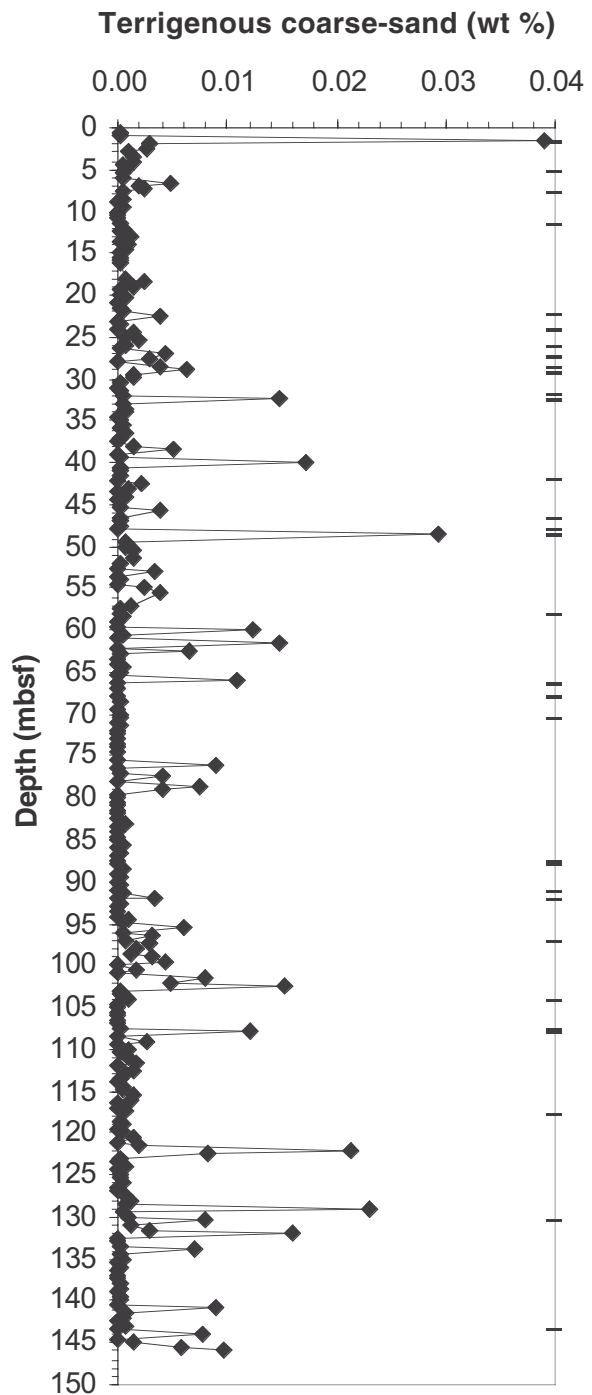
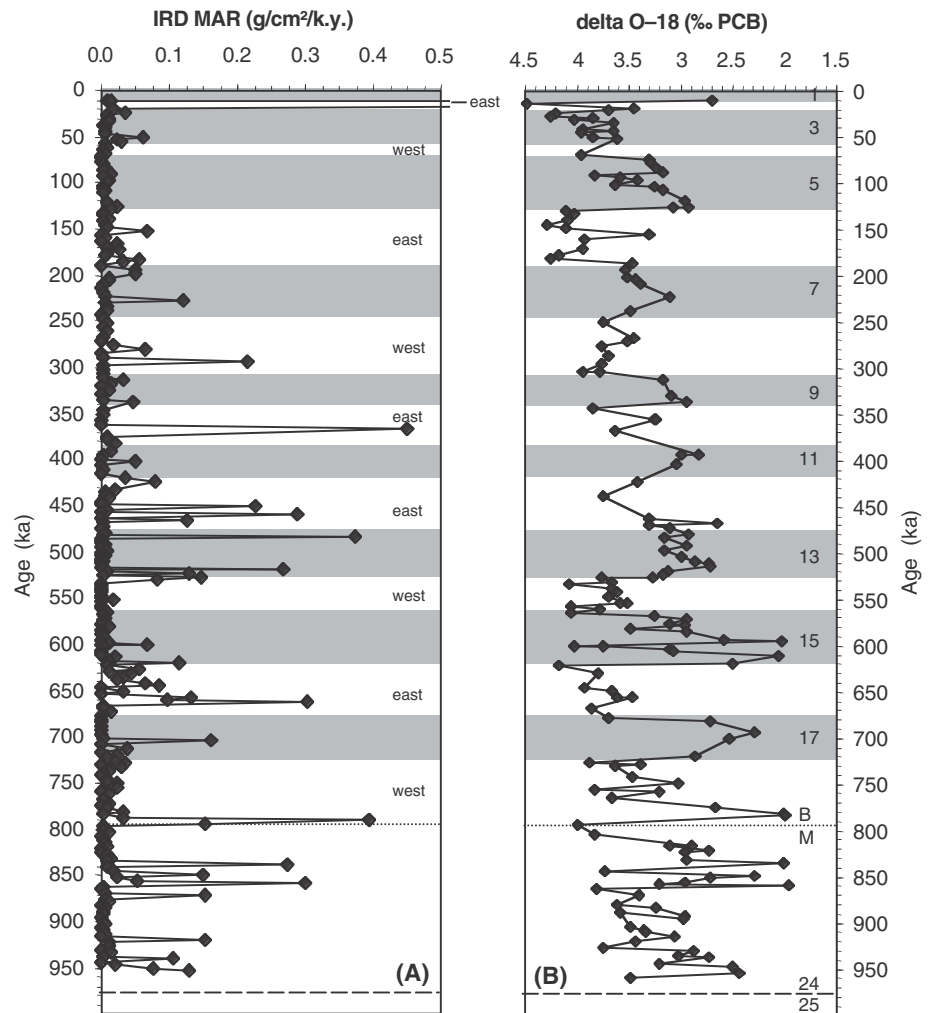


Fig. 2. Terrigenous coarse sand abundance plotted against downcore depth (mbsf = meters below sea floor) for Site 919. Horizontal bars represent the occurrence of dropstones >0.2 cm on the cut surfaces of cores (Shipboard Scientific Party, 1994b).

Fig. 3. Site 919 a) IRD MAR plotted against calculated age. The IRD MAR value at 11.92 ka is 2.29 g/cm²/ky. The position of the polar front according to Koç and Flower (1998) relative to site 919 is indicated by “east” or “west” for glacial Stages 2–18. “East” means the polar front was east of site 919, “west” means the polar front was west of site 919. b) Oxygen isotope Stages from Flower (1998). Stages 1–18 are represented by shaded horizontal bars and are numbered to the right. Stages 19–23 are not defined. Stage boundary 24/25 is indicated by a dashed line. The Brunhes/Matuyama magnetic boundary is indicated by the dotted line.



bulk MAR (which is the product of the linear sedimentation rate (LSR) and the dry bulk density (DBD) of that sediment) by the weight percent of the terrigenous coarse sand fraction such that:

$$\text{LSR [cm/k.y.]} \times \text{DBD [g/cm}^3\text{]} \times \text{terrigenous coarse sand wt\% [a decimal fraction]} = \text{IRD MAR [g/cm}^2\text{/k.y.]}$$

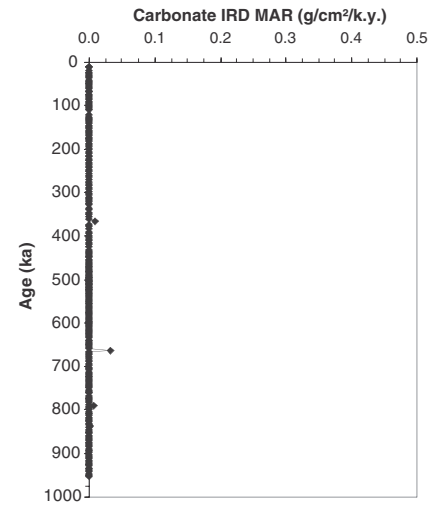
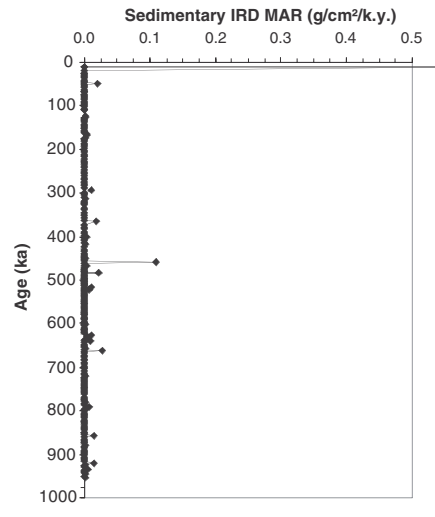
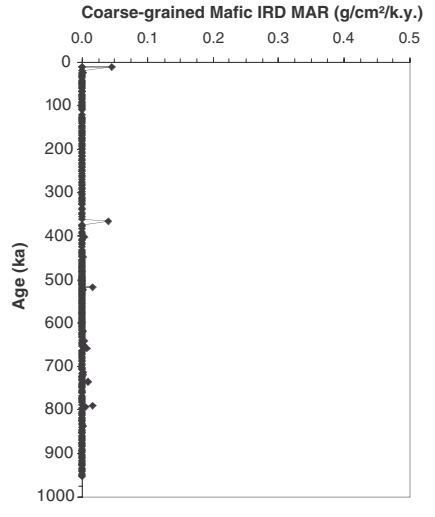
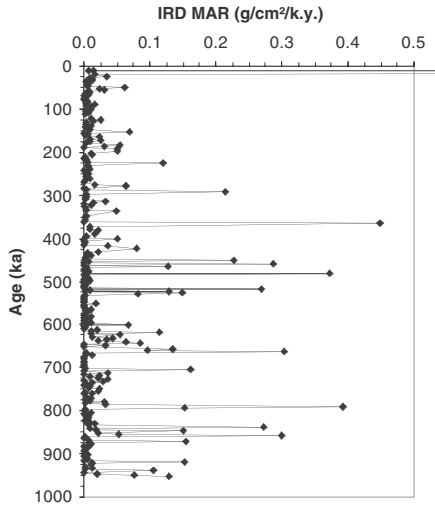
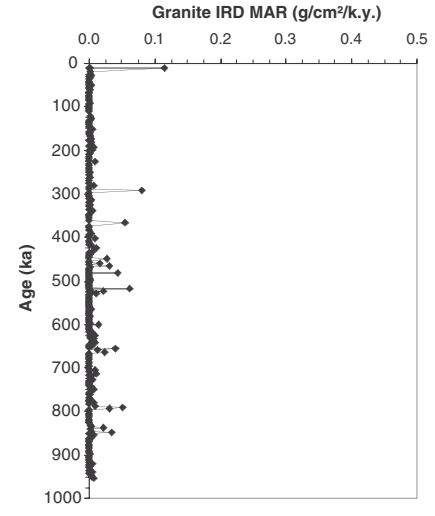
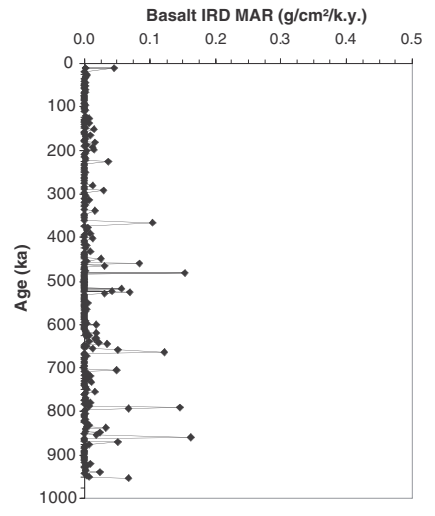
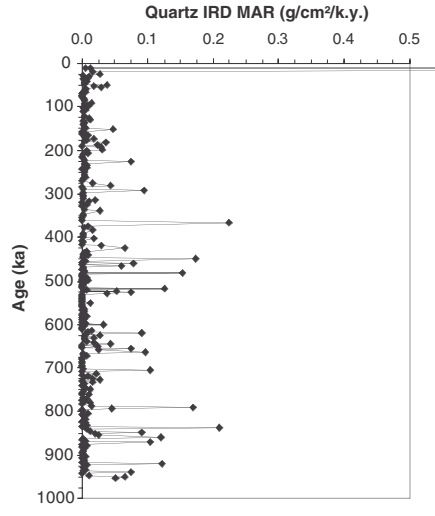
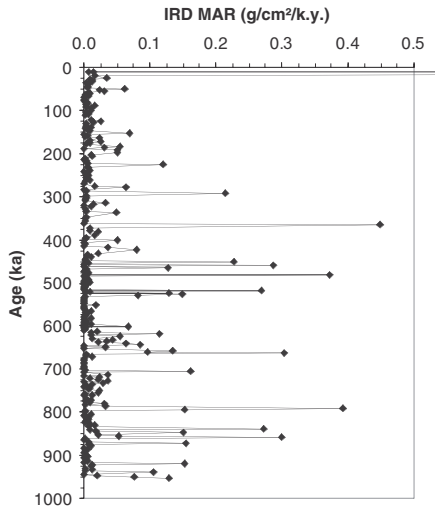
DBD values were taken from the nearest shipboard index properties sample listed in Shipboard Scientific Party (1994b). The MAR of each IRD grain type is calculated by multiplying the total IRD MAR by the abundance of each grain type within the total population of IRD grains.

Results

IRD MAR values range from 0 to ~2.3 g/cm²/k.y. (0 and ~0.04 wt%; Figs 2–3) at site 919, with the highest

IRD flux occurring at ~11.9 ka (1.44 mbsf) during oxygen-isotope Stage 2. This highest IRD flux results largely because of the very high sedimentation rate (75 cm/kyr) between 10 and 12 ka, in combination with an IRD abundance peak of ~0.04%. With the exception of this IRD MAR peak, large amplitude fluctuations of IRD flux primarily are older than ~250 ka (oxygen-isotope Stage 7). These older IRD MAR peaks have maximum values between 0.2 and 0.5 g/cm²/k.y. Overall there is no clear correlation between the pattern of IRD flux to site 919 and marine oxygen-isotope stages; peaks in IRD MARs occur not only during glacial stages, but also during interglacial stages and at stage boundaries.

The depths at which IRD maxima occur and the depths at which larger dropstones (i.e., clasts > 0.2 cm; Fig. 2) were identified on cut surfaces of the cores show some similarities, but not an exact correlation. Many episodes of increased IRD input to site 919 (e.g., between 75–80 mbsf) are not recorded in the dropstone record, but are only revealed through more continu-



ous analysis of sand-sized IRD as was done in this study. X-radiograph analysis of the cores would likely improve the correlation between the dropstone and coarse-sand IRD records. In addition, though less common, are intervals (e.g., 87–88 mbsf) where dropstones are present without a corresponding sand-size IRD maximum. This suggests that some ice-rafting events are not represented in the sand-size IRD record, because of the temporal resolution introduced by our sampling interval.

Quartz, basalt, and granitic/coarse-grained felsic are the three most abundant IRD grain types at site 919 (Fig. 4); MARs of quartz IRD range from 0 to 1.5 g/cm²/k.y., MARs of basalt range from 0 to 0.16 g/cm²/k.y., and MARs of granite/coarse grained felsic range from 0 to 0.11 g/cm²/k.y. Peaks in the total IRD MAR record primarily are produced by an increase in the MARs of one or more of these dominant components. With the exception of a few isolated peaks (e.g., the sedimentary IRD peak at ~11.9 ka), the MARs of coarse-grained mafic IRD and sedimentary rock fragments IRD are low to zero throughout the site 919 record.

Discussion

IRD Provenance and Iceberg Dispersal

The composition of sand-size IRD at site 919 is consistent with the lithologies of larger dropstones recorded during shipboard core description (Shipboard Scientific Party 1994b), with the known onshore geology of southeast and central east Greenland (Bridgewater et al. 1976; Larsen 1980), and with the composition of modern and Pleistocene IRD from East Greenland (Molnia 1983; Linthout et al. 2000). The most likely source area for the granitic/coarse-grained felsic IRD is the Precambrian igneous and meta-igneous crystalline basement (predominantly gneiss and granite) of southeast Greenland, located immediately southwest, west, and northwest of site 919. Basaltic IRD was probably derived from Tertiary flood basalts exposed between Scoresby Sund and Kap Gustav Holm (Fig. 1; Deer 1976; Larsen 1980), ~500 km or more north and northwest of site 919.

The widespread distribution of quartz in the lithologies exposed in East Greenland limits the value of quartz as a provenance indicator; however, some of the quartz grains at site 919 are hematite stained, suggesting that quartz IRD was in part derived from red

beds in east Greenland. Sedimentary rock fragments, however, are poorly represented at site 919, with clastic grains dominating those that are present. Possible sources of clastic sedimentary IRD along the East Greenland coast include scattered pre-volcanic deposits, such as Tertiary marine to shallow water sedimentary sequences at Kap Gustav Holm, and Cretaceous to earliest Paleocene marine to shallow marine sediments in the Kangerdlugssuaq area. These possible sources are problematic, however, because both generally are protected from erosion by thick basaltic caps (Larsen 1980). Another possibility is that sedimentary rock fragments were transported from fjords cut into the Paleozoic “Caledonian molasse” (Haller 1971) exposed in the Caledonian fold belt in northeastern Greenland (Larsen et al. 1994; Henriksen & Higgins 1976). These exposures, however, extend far enough north that colder glacial conditions and more extensive shore-fast sea ice may have limited their effectiveness as IRD sources (Funder et al. 1998). A final possible source was identified by Linthout et al. (2000), who reported the presence of a red quartzitic dropstone in a surface grab from the SE Greenland continental margin. They tentatively linked this dropstone to Lower Mesozoic sedimentary rocks in northern Jameson Land, south of 72°N. As with the sources of basaltic IRD grains, these possible sources of sedimentary IRD grains all lie 500 km or more north of site 919.

A comparison of the site 919 IRD data and the IRD composition and abundance data from more shoreward locations (ODP sites 914–918; Fig. 1; Shipboard Scientific Party 1994a; Kudless-St. John 1999) indicates that Site 919 had lower total IRD MARs and received less felsic IRD (quartz and granitic/c.g. felsic rock fragments) than the more landward sites, located ~130 km to the west. Thus, the IRD composition further offshore (site 919) was influenced relatively more by distant, yet directly up-current iceberg calving localities than by nearby iceberg sources directly to the west. Icebergs that transported material eastward from the felsic crystalline rocks exposed along the SE Greenland coast experienced greater melting and/or were caught in the strong, southward-flowing East Greenland Current before reaching Site 919, thus reducing both the total IRD input and the input of felsic IRD to this site. Icebergs originating from basaltic exposures, however, entered the EGC farther to the north, and some of these icebergs were carried offshore by the time they reached 63°N latitude. This resulted in similar basaltic IRD MARs at sites 918 and 919, even though the relative importance of basaltic IRD in the total IRD population is much greater at Site 919.

Peaks in the total IRD MAR profile of Site 919 generally result from synchronous increases in both the quartz and basalt IRD MARs, and secondarily from

←
Fig. 4. Component IRD flux (IRD MAR) profiles. Replicate total IRD MAR profiles are included on the left of each row for comparison.

increases in granitic/coarse-grained felsic IRD MARs (Fig. 4). This covariation in the MARs of different IRD grain types, derived from different locations along the SE Greenland coast, suggests that IRD supply from geographically and geologically distinct source regions varied synchronously during much of Pleistocene. In light of these IRD provenance interpretations, the covariation in the MARs of different IRD grain types indicates that the region of Precambrian igneous and meta-igneous crystalline basement in south-east Greenland, the Tertiary flood basalt region between Scoresby Sund and Kap Gustav Holm, and perhaps Jameson Land and the fjords in the southern Caledonides experienced similar iceberg release histories during the Pleistocene. The work by Funder et al. (1998) examined the glacial history from Scoresby Sund north to ~75°N during the past ~240 ky, but equivalent data are not available for the region south of Scoresby Sund. As a result, independent data are not available to evaluate: 1) Middle to Late Pleistocene glacial conditions south of Scoresby Sund, where important IRD source areas to Site 919 are located; or 2) glacial/interglacial conditions older than 240 ka anywhere along the SE Greenland coast.

Input of sedimentary rock fragments to site 919 as IRD was significant only during the last deglaciation (Fig. 4; Stage 2). Large increases in the fluxes of quartz grains and sedimentary rock fragments were responsible for the very high total IRD flux at 11.9 ka. An increase in the sedimentary rock fragment IRD flux is also seen at site 918 in the late Pleistocene (Kudless-St. John 1999). This implies a shift in the relative importance of sedimentary source areas towards the end of the last glaciation, whereby total IRD supply increased greatly in response to iceberg-calving almost entirely from areas where sedimentary bedrock was exposed. The two nearest areas with outcrops of sedimentary rocks are the Kangerdlugssuaq/Kap Gustav Holm region and Jameson Land, just north of Scoresby Sund. On the continental margin near Kangerdlugssuaq, sedimentation decreased after ~15 ka (Andrews et al. 1996), attributed to retreat of the ice from the shelf break at that time. During that retreat, the calving ice front may have passed briefly through a position more directly upcurrent from site 919, thereby increasing the input of sedimentary rock IRD as recorded at ~11.9 ka. Contemporaneous IRD records from the continental slope off Scoresby Sund show significant, but episodic, IRD inputs from ~29 ka to ~12 ka, but the decrease at 12 ka is attributed to deglaciation of the outer fjord basins (Funder et al. 1998). As a result, this more glacial proximal record suggests that the increase in sedimentary rock IRD at site 919 at ~11.9 ka was not sourced from the Jameson Land/Scoresby Sund region.

Timing of Ice-Rafting Within Glacial-Interglacial Cycles

A planktonic foraminifera-based oxygen-isotope stratigraphy for Site 919 (Flower 1998) provides a well-constrained time framework for calculating the IRD MAR record at that site, and also supplies valuable paleoclimatic data for the Irminger Basin since 960 ka. The site 919 oxygen isotope and IRD MAR records are both climatic indicators, but respond to different spatial scales of variation (i.e., global vs. local climate signals), so a comparison of the two reveals the response of glacial ice in SE Greenland to global climate forcing. The overall poor correlation between site 919 IRD MAR peaks and global $\delta^{18}\text{O}$ stages indicates that local controls on iceberg production, transport, and melting had an overriding influence on IRD flux to site 919 during the last 960 kyr (Fig. 3).

The various local controls that influenced the rate of IRD supply to the Irminger Basin are difficult to isolate and assess independently. Here we will explicitly consider the effects of the paleo-position of the Polar Front, the boundary between cooler high-latitude surface waters and warmer surface waters derived from the North Atlantic, while also considering the potential roles of nearshore and regional sea ice cover. The position of the Polar Front is important because it determines the position where most icebergs melt (e.g. Ruddiman 1977). Based on a study of diatom assemblages at site 919, Koç & Flower (1998) inferred east-west shifts of the Polar Front across the western Irminger Basin during the last 1 My (Fig. 3). They concluded that glacial Stages 2, 6, 10, 12, and 16 were relatively cold, causing the Polar Front to migrate east of site 919. Although limited to a shorter record, Funder et al. (1998) support this interpretation, specifically by concluding that Stage 6 was the most extensive glaciation seen in the East Greenland terrestrial record during the past 240 ky. Conversely, milder climates were interpreted to have prevailed during glacial Stages 4, 8, 14, 18, so that the Polar Front was located west of site 919 (Koç & Flower 1998). Funder et al. (1998), however, interpreted Stage 4 in the Scoresby Sund region as a long-lasting event, with ice extending onto the inner continental shelf for more than 50 ky. The interpretation of milder glacials compares favorably with our IRD flux record, in that IRD MARs at site 919 were low during Stages 4, 8, 14, and 18. Presumably site 919 was beyond the geographic limit of significant iceberg melting (i.e., the Polar Front) at these times. In addition, if stages 4, 8, 14, and 18 were warmer glacials, as Koç & Flower (1998) suggested, then glacial ice may have retreated from the coastal regions, resulting in reduced iceberg production at these times. Alternatively, as interpreted by Funder et al. (1998) for

Stage 4 marine sediments near Scoresby Sund, extensive shorefast sea ice cover at the iceberg sources may have prevented iceberg drift and IRD delivery to the offshore site 919.

Site 919 was within the normal limit of iceberg rafting during glacial stages 2, 6, 10, 12, and 16, assuming Koç & Flower (1998) were correct in concluding that the Polar Front was east of site 919 during these glacial stages. IRD supply to site 919 was variable, however, during these times; high rates of IRD supply occurred during Stages 2, 12, and 16, but rates were low during Stages 6 and 10. These differences may be explained by variations in the distribution of sea ice, both across site 919 and as shorefast ice near the iceberg sources. Koç & Flower (1998) suggested that sea ice extended across the location of site 919 during stages 6 and 10, which would have limited the transport of debris-laden icebergs to the area. In contrast, we suggest that permanent regional sea ice was less extensive during glacial Stages 2, 12, and 16, thus allowing the transport of icebergs and IRD to site 919. Alternatively, varying spatial and temporal distributions of nearshore sea ice at the iceberg sources also may have affected IRD supply to site 919. For example, IRD contents off Scoresby Sund are lower in Stage 6 sediments than in Stage 2 deposits, attributed to the effects of long-lasting shorefast ice during Stage 6 (Funder et al. 1998). The shorefast ice must have been geographically limited during stage 6, however, because IRD contents in stage 6 marine sediments north of Scoresby Sund (Funder et al. 1998) are as high as, or higher than, the IRD contents in stage 2 sediments in that area.

A final possible regional control on the IRD record at site 919 is temporal variation in the availability of easily eroded material within the glaciated source areas. For example, it is interesting to note that the highest IRD MARs within glacial Stages 16, 12, 10, and 8 each occurred at the onset of glaciation, with IRD MARs decreasing as each glaciation proceeded. This repeated pattern suggests that easily eroded material, weathered during the preceding interglacial, was rapidly removed by the initial glacial advance. After this erodible cover was removed, then the debris load within the glaciers was reduced, even though total ice volume may have increased. Alternatively, the decrease in IRD supply through these glacial stages may record either: 1) a change in the glacial terminus regime as each glaciation intensified, from conditions initially like those presently found near Scoresby Sund to conditions equivalent to those presently found north of ~78°N (Funder et al. 1998; Reeh et al. 1999); or 2) the development of more permanent nearshore sea ice at the iceberg source regions.

This pattern, where IRD abundance decreases through an older glacial stage, is more evident in the

MAR record for basaltic IRD than in the MAR record for granitic IRD, suggesting either that: 1) the basaltic source rocks were more susceptible than the granitic source rocks to weathering during interglacials; or 2) glacial terminus regimes and/or nearshore sea ice extents were more variable in the Kap Gustav Holm/Scoresby Sund region than further to the south. It is also interesting to note that the transitions into Stages 16, 12, 10 and 8, which show maximum IRD MARs at the onset of glaciation, are marked by relatively large amplitude changes in the benthic oxygen isotope record (Bradley 1999, Fig. 6.11). The large-amplitude oxygen isotope shifts suggest intensified climatic changes, from relatively equable climates suitable for extensive weathering to relatively intense glaciations. In contrast, the transition from Stage 15 into Stage 14 is marked by a relatively low amplitude change in the benthic oxygen isotope record (Bradley 1999; Fig 6.11), suggesting a less drastic climatic shift, which is consistent with reduced weathering during interglacial Stage 15 and reduced IRD influx at the start of glacial Stage 14 (Fig. 3).

The IRD record at a location is affected by both global climate and regional controls. Our data from site 919 suggests that iceberg release to the open ocean from glaciers throughout SE Greenland fluctuated synchronously during the last 1 My, with the resulting record of IRD input also affected by glacial terminus regime, ocean circulation, sea surface temperature patterns, sea-ice distribution, and availability of easily eroded surficial material. Because of these complications, the IRD record from SE Greenland does not correlate well with the global oxygen isotope record, which is strongly influenced by Pleistocene variations in the Laurentide Ice Sheet. Dowdeswell et al. (1999) concluded that the dynamics of Quaternary ice sheets surrounding the Nordic Seas were different from the dynamics of glaciers draining the Laurentide Ice Sheet. Our data suggest that this observation is also valid for the ice sheets in SE Greenland.

Conclusions

1) Compositional analyses indicate that the major source regions for IRD found off SE Greenland were the Precambrian igneous and meta-igneous crystalline basement (predominantly gneiss and granite) of southeast Greenland and the Tertiary flood basalts located further north along the East Greenland coast (but south of Scoresby Sund). Temporal covariations in the IRD MARs of provenance-distinctive grain types suggest that these source areas experienced similar iceberg release histories during the Pleistocene.

2) The history of IRD input off SE Greenland is dominated by local, rather than global, climatic and distributional controls, as no distinct relationship can be drawn between the timing of IRD MAR maxima at this site and oxygen-isotope defined glacial-interglacial cycles.

Acknowledgments

The authors gratefully acknowledge Walter Hale and Alex Wuelbers at the Bremen Core Repository for their assistance with sampling, and Jessica Albrecht, Chris Brown, Rich Jacko, Maura Metheny, and Attiya Mobin-Uddin for their assistance with sample processing. The constructive comments of Ben Flower, Joe Morley and John Andrews and one anonymous reviewer helped improve this manuscript. This work was funded by a JOI-USSSP post-cruise research grant.

References

- Andrews, J.T. 2000: Icebergs and iceberg rafted detritus (IRD) in the North Atlantic: facts and assumptions. *Oceanography* 13, 100–108.
- Andrews, J.T., Cooper, T.A., Jennings, A.E., Stein, A.B. & Erlenkeusen, H. 1998: Late Quaternary iceberg-rafted detritus events on the Denmark Strait-southeast Greenland continental slope (~65°N) related to North Atlantic Heinrich events. *Marine Geology* 149, 211–228.
- Andrews, J.T., Smith, L.M., Preston, R., Cooper, T. & Jennings, A.E. 1997: Spatial and temporal patterns of iceberg rafting (IRD) along the East Greenland margin, ca. 68°N, over the last 14 cal ka. *Journal of Quaternary Science* 12, 1–13.
- Andrews, J.T., Jennings, A.E., Cooper, T., Williams, K.M. & Mienert, J. 1996: Late Quaternary sedimentation along fjord to shelf (trough) transect, East Greenland (ca. 68°N). In Andrews et al. (eds.) *Late Quaternary Paleooceanography of the North Atlantic Margins*, Geological Society Special Publication 111, 153–167.
- Bennike, O. & Bøcher, J. 1990: Forest-tundra neighboring the north pole: plant and insect remains from the Plio-Pleistocene Kap Kobenhavn Formation, North Greenland. *Arctic* 43, 331–338.
- Bond, G., Heinrich, H., Huon, S., Broecker, W., Labeyrie, L., Andrews, J., McManus, L., Clasen, S., Tedesco, K., Kantschik, R., Simet, C. & Klas, M. 1992: Evidence for massive discharges of icebergs into the glacial North Atlantic. *Nature* 360, 245–249.
- Bradley, R. 1999: *Paleoclimatology: Reconstructing Climates of the Quaternary* (2nd ed.). 613 pp. New York: Harcourt.
- Bridgwater, D., Keto, L., McGregor, V.R. & Meyers, J.S. 1976: Nagssugtoqidian mobile belt in East Greenland. In Escher, A. & Watt, W.S. (eds.) *Geology of Greenland*, 18–75, Geological Survey of Greenland, Copenhagen.
- Bridgwater, D., Keto, L., McGregor, V.R. & Myers, J.S. 1976: Archaean gness complex of Greenland. In Escher, A. & Watt, W.S. (eds) *Geology of Greenland*, 19–73. The Geological Survey of Greenland, Copenhagen.
- Christiansen, F.G., Larsen, H.C., Marcussen, C., Hansen, K., Krabbe, H., Larsen, L.M., Piasecki, S., Stemmerik, L. & Watt, W.S. 1992: Uplift study of the Jameson Land basin, East Greenland. *Norsk Geologisk Tidsskrift* 72, 291–294.
- Clift, P.D., Carter, A. & Hurford, A.J. 1996: Constraints on the evolution of the East Greenland Margin: evidence from detrital apatite in offshore sediments. *Geology* 24, 1013–1016.
- Clift, P.D. & Fitton, J. G. 1998: Trace and rare earth element chemistry of volcanic ashes from Sites 918 and 919: implications for Icelandic volcanism. In Larsen, H.C., Saunders, A.D., Clift, P.D. et al. (eds) *Proceedings of the Ocean Drilling Program, Scientific Results 152*, 67–84, Ocean Drilling Program, College Station, TX.
- Conolly, J.R. & Ewing, M. 1970: Ice-rafted detritus in northwest Pacific deep-sea sediments. In Hayes, J.D. (ed.) *Geological Investigations of the North Pacific*, Geological Society of America Memoir 126, 219–231.
- Deer, W.A. 1976: Tertiary igneous rocks between Scoresby Sund and Kap Gustav Holm, East Greenland. In Escher, A. & Watt, W.S. (eds) *Geology of Greenland*, 404–429. The Geological Survey of Greenland, Copenhagen.
- Dowdeswell, J.A., Elverhoi, A., Andrews, J.T. & Hebbeln, D. 1999: Asynchronous deposition of ice-rafted layers in the Nordic seas and North Atlantic Ocean. *Nature* 400, 348–251.
- Feyling-Hanssen, R.W., Funder, S. & Petersen, K.S. 1982: The Lodin Elv Formation; a Plio-Pleistocene occurrence in Greenland. *Bulletin of the Geological Society of Denmark* 31, 81–104.
- Flower, B. 1998: Mid- to Late Quaternary stable isotope stratigraphy and paleoceanography at site 919 on the southeast Greenland margin. In Larsen, H.C., Saunders, A.D., Clift, P.D. et al. (eds) *Proceedings of the Ocean Drilling Program, Scientific Results 152*, 243–248. Ocean Drilling Program, College Station, TX.
- Funder, S., Hjort, C., Landvik, J.Y., Nam, S., Reeh, N. & Stein, R. 1998: History of a stable ice margin – East Greenland during the Middle and Upper Pleistocene. *Quaternary Science Reviews* 17, 77–123.
- Funder, S. 1989: Quaternary geology of East Greenland, in Fulton, R.J. (ed.) *Quaternary Geology of Canada and Greenland*, 756–763. Geological Survey of Canada, Geology of Canada no. 1.
- Funder, S., Abrahamsen, N., Bennike, O. & Feyling-Hanssen, R. W. 1985: Forested arctic: evidence from north Greenland. *Geology* 13, 542–546.
- Goldschmidt, P.M. 1995: Accumulation rates of coarse-grained terrigenous sediment in the Norwegian-Greenland Sea: signals of continental glaciation. *Marine Geology* 128, 137–151.
- Haller, J. 1971: *Geology of the East Greenland Caledonides*. 413 pp. London: Wiley Interscience.
- Henriksen, N. & Higgins, A.K. 1976: East Greenland Caledonian fold belt. In Escher, A. and Watt, W.S. (eds) *Geology of Greenland*, 182–247. The Geological Survey of Greenland, Copenhagen.
- Jansen, E., Fronval, T., Rack, F. & Channell, J. 2000: Pliocene-Pleistocene ice rafting history and cyclicity in the Nordic Seas during the last 3.5 Myr. *Paleoceanography* 15, 709–721.
- Jansen, E., Sjöholm, J., Bleil, U. & Erichsen, J. A. 1990: Neogene and Pleistocene glaciations in the Northern Hemi-

- sphere and late Miocene-Pliocene global ice volume fluctuations: evidence from the Norwegian Sea. In Bleil, U. & Thiede, J. (eds) *Geological History of the Polar Oceans: Arctic Verses Antarctic*, 677–705, Kluwer, Dordrecht.
- Koç, N. & Flower, B.P. 1998: High resolution diatom biostratigraphy and paleoceanography of site 919 from the Irminger Basin. In Larsen, H.C., Saunders, A.D., Clift, P.D., et al. (eds) *Proceeding of the Ocean Drilling Program Scientific Results 152*, 209–220. Ocean Drilling Program, College Station, TX.
- Krissek, L.A. 1999: Data report: mass accumulation rates and composition of Neogene ice-rafted debris; Site 919, Irminger Basin. In Larsen, H.C., Duncan, R.A., Allen, J.F. & Brooks, K. (eds) *Proceedings of the Ocean Drilling Program, Scientific Results 163*, 157–161. Ocean Drilling Program, College Station, TX.
- Krissek, L.A. 1995: Late Cenozoic ice-rafting records from ODP Leg 145 sites in the North Pacific: Late Miocene onset, late Pliocene intensification, and Plio-Pleistocene events. In Rea, D.K., Basov, I.A., Scholl, D.W., Allan, J.F., et al. (eds) *Proceedings of the Ocean Drilling Program Scientific Results 145*, 179–194. Ocean Drilling Program, College Station, TX.
- Kudless-St. John, K.E. 1999: Data report: site 918 IRD mass accumulation rates record, late Miocene-Pleistocene. In Larsen, H.C., Duncan, R.A., Allan, J.F., & Brooks, K. (eds) *Proceedings of the Ocean Drilling Program, Scientific Results 163*, 163–166. Ocean Drilling Program, College Station, TX.
- Lacasse, C. Werner, R., Paterne, M., Sigurdsson, H., Carey, S. & Pinte, G. 1998: Long-range transport of Icelandic tephra to the Irminger Basin, Site 919. In Larsen, H.C., Saunders, A.D., Clift, P.D. et al. (eds) *Proceedings of the Ocean Drilling Program, Scientific Results 152*, 51–66. Ocean Drilling Program, College Station, TX.
- Larsen, H.C. 1980: Geological perspectives of the East Greenland continental margin. *Bulletin of the Geological Society of Denmark* 29, 77–101. Larsen, H.C., 1984: *Geology of the East Greenland Shelf*. In Spencer, A.M., Johnsen, S.O., Moerk, A., Nysaether, E., Songstad, P. & Spinnangr, A. (eds) *Petroleum Geology of the North European Margin*, 329–339. Graham and Trotman, London, United Kingdom.
- Larsen, H.C. 1990: The East Greenland Shelf. In Grantz, A., Johnson, G.L. & Sweeney, J.F. (eds) *The Arctic Ocean Region*, 185–210, Geological Society of America, *Geology of North America Series L*.
- Larsen, H.C., Saunders, A.D., Clift, P.D., Beget, J., Wei, W., Spezzaferri, S. & ODP Leg 152 Scientific Party 1994: Seven million years of glaciation in Greenland. *Science* 264, 952–955.
- Linthout, K., Troelstra, S.R. & Kuijpers, A. 2000: Provenance of coarse ice-rafted detritus near the SE Greenland margin. *Netherlands Journal of Geosciences* 79, 109–121.
- Lysa, A. & Landvik, J.Y. 1994: Cyclic changes in the sedimentary environment during the last interglacial/glacial cycle; coastal Jameson Land, East Greenland. *Palaeogeography, Palaeoclimatology, Palaeoecology* 112, 143–156.
- Molnia, B.F. 1983: Distal glacial-marine sedimentation: abundance, composition, and distribution of North Atlantic ocean Pleistocene ice-rafted sediment. In Molnia, B.F. (ed.) *Glacial-Marine Sedimentation*, 593–626, Plenum, New York.
- Reeh, N., Mayer, C., Miller, H., Thomsen, H.H. & Weidick, A. 1999: Present and past climate control on fjord glaciations in Greenland: implications for IRD-deposition in the sea. *Geophysical Research Letters* 26, 1039–1042.
- Reeh, N., 1991: Parameterization of melt rate and surface temperatures on the Greenland ice sheet. *Polarforschung* 59, 113–128.
- Reeh, N. 1989; Dynamic and climatic history of the Greenland Ice Sheet. In Fulton R.J. (ed.) *Quaternary Geology of Canada and Greenland*, 795–822. Geological Survey of Canada, Geology of Canada.
- Ruddiman, W.F. 1977: Late Quaternary deposition of ice-rafted sand in the subpolar North Atlantic (lat 40° to 65°N). *Geological Society of America Bulletin* 88, 1813–1827.
- Shipboard Scientific Party 1994a: Shelf Stratigraphic Synthesis. In Larsen, H.C., Saunders, A.D., Clift, P.D. et al. (eds) *Proceeding of the Ocean Drilling Program Initial Reports 152*, 159–176. Ocean Drilling Program, College Station, TX.
- Shipboard Scientific Party 1994b: Site 919. In Larsen, H.C., Saunders, A.D., Clift, P.D. et al. (eds) *Proceeding of the Ocean Drilling Program Initial Reports 152*, 257–278. Ocean Drilling Program, College Station, TX.
- Shipboard Scientific Party, 1994c: Summary and principal results. In Larsen, H.C., Saunders, A.D., Clift, P.D. et al. (eds) *Proceeding of the Ocean Drilling Program Initial Reports 152*, 279–292. Ocean Drilling Program, College Station, TX.
- Spezzaferri, S. 1998: Planktonic foraminifera biostratigraphy and paleoenvironmental implications of Leg 152 sites (east Greenland margin). In Larsen, H.C., Saunders, A.D., Clift, P.D. et al. (eds) *Proceedings of the Ocean Drilling Program, Scientific Results 152*, 161–190. Ocean Drilling Program, College Station, TX.
- St. John, K.E.K. & Krissek, L.A. 1999: Regional patterns of Pleistocene ice-rafted debris flux in the North Pacific. *Paleoceanography* 14, 653–662.
- Stein, R., Nam, S.I., Grobe, H. & Hubberten, H. 1996: Late Quaternary glacial history and short-term ice-rafted debris fluctuations along the East Greenland continental margin. In Andrews, J.T., Austin, W.E., Bergaten, H. & Jennings, A.E. (eds) *The Late Quaternary Paleocceanography of North American Margins*, GSA Special Publication, 111, 135–151.
- Wei, W. 1998: Calcareous nannofossils from the southeast Greenland margin: biostratigraphy and paleoceanography. In Larsen, H.C., Saunders, A.D., Clift, P.D. et al. (eds): *Proceedings of the Ocean Drilling Program Scientific Results 152*, 147–160. Ocean Drilling Program, College Station, TX.